Estimating stress state along the San Jacinto and southern San Andreas faults on the eve of past ground rupturing earthquakes and implications for current stress state

Report for SCEC Award #22030
Submitted January 2024

Investigators: Dr. Michele L. Cooke and PhD Candidate Emery Anderson-Merritt

Table of Contents

I. Project Overview

A. Abstract

In the box below, describe the project objectives, methodology, and results obtained and their significance. If this work is a continuation of a multi-year SCEC-funded project, please include major research findings for all previous years in the abstract. (Maximum 250 words.)

Estimating the evolving state of stress in a fault system can help us constrain the conditions that may have generated previous ground-rupturing earthquakes and constrain initial conditions for dynamic rupture models of large earthquakes. We use forward numerical models that incorporate 3D complex configuration of active faults in southern California to estimate shear tractions on the southern San Andreas and San Jacinto fault systems since 1000 CE. We include the accumulation of traction due to tectonic loading, long-term viscoelastic relaxation of stress within the crust, and effects of nearby earthquakes. To simulate interseismic shear traction accumulation we use a two-step back slip approach to estimate linear interseismic loading rate and subtract from it the effect of viscoelastic stress relaxation. We simulate ground-rupturing earthquakes by assigning a tapered stress drop along the rupture length based on the earthquake extents from Scharer & Yule (2020), estimating the magnitude of this stress drop by best fit to available geologic data. We combine these models to estimate evolved tractions assuming overall ~0.75 MPa stress drops for large ground rupturing earthquakes, which is consistent with slip per event data. Over a long timeframe, stress relaxation reduces traction uncertainties arising from earthquake timing and stress drop uncertainty. Uncertainties of viscosity have larger impact than stress drop or earthquake timing. Larger ruptures are associated with greater accumulation of pre-earthquake traction. This new modeling approach provides estimates of shear tractions that are unavailable from direct measurements.

B. SCEC Annual Science Highlights

Each year, the Science Planning Committee reviews and summarizes SCEC research accomplishments, and presents the results to the SCEC community and funding agencies. Rank (in order of preference) the sections in which you would like your project results to appear. Choose up to 3 working groups from below and re-order them according to your preference ranking.

Stress and Deformation Through Time (SDOT)
San Andreas Fault System
Earthquake Geology

C. Exemplary Figure

Select one figure from your project report that best exemplifies the significance of the results. The figure may be used in the SCEC Annual Science Highlights and chosen for the cover of the Annual Meeting Proceedings Volume. In the box below, enter the figure number from the project report, figure caption and figure credits.

Figure 3: Pre-earthquake tractions from Monte Carlo simulations using elastic and inelastic rheology incomplete stress drop scenarios. Minimum pre-earthquake tractions increase with rupture length.

D. SCEC Science Priorities

In the box below, please list (in rank order) the SCEC priorities this project has achieved. See *https://www.scec.org/research/priorities* for list of SCEC research priorities. *For example: 6a, 6b, 6c*

1c. Develop an integrated quasi-static modeling framework incorporating information in the community models, and apply it to estimate the stress field and its uncertainties, to be updated periodically.

1d. Quantify stress heterogeneity on faults at different spatial scales, correlate the stress concentrations with asperities and geometric complexities, and model their influence on rupture initiation, propagation, and arrest.

2a. Determine how off-fault deformation contributes to geodetic estimates of strain accumulation and what fraction of seismic-moment accumulation is relaxed by aseismic processes. accounting for observational and modeling uncertainties.

E. Intellectual Merit

How does the project contribute to the overall intellectual merit of SCEC? For example: How does the research contribute to advancing knowledge and understanding in the field and, more specifically, SCEC research objectives? To what extent has the activity developed creative and original concepts?

In this study, we estimate the evolving and pre-earthquake along-strike shear tractions along the San Andreas and San Jacinto faults since ~1000 CE. Models with overall stress drop of ~0.75 MPa produce slip per event that are consistent with geologic data and models with upper crustal viscosity of 10^{20} Pa-sec or greater produce traction histories that are consistent with geologic data. We also investigate the impacts of uncertainty in earthquake timing, upper crustal viscosity and stress drop on shear traction estimates. Uncertainties in crustal viscosity have the greater impact on shear tractions followed by stress drop uncertainties. While the earthquake timing uncertainties are large, they do not impact the shear traction estimates as much as other uncertainties. Estimates of the fault shear tractions through time and over several earthquake cycles reveal potential conditions that preceded previous ground-rupturing earthquakes and can provide initial conditions for dynamic rupture models. Our findings show that longer ruptures are associated with greater accumulated shear traction prior to the earthquake.

F. Broader Impacts

How does the project contribute to the broader impacts of SCEC as a whole? For example: How well has the activity promoted or supported teaching, training, and learning at your institution or across SCEC? If your project included a SCEC intern, what was his/her contribution? How has your project broadened the participation of underrepresented groups? To what extent has the project enhanced the infrastructure for research and education (e.g., facilities, instrumentation, networks, and partnerships)? What are some possible benefits of the activity to society?

The pre-earthquake tractions along the San Andreas and San Jacinto faults can be used as initial conditions for dynamic rupture models. This product would be a significant refinement for models that simulate past earthquake events and yield insight into the conditions that generate damaging earthquakes. This project supports both a UMass PhD candidate, Emery Anderson-Merritt, who is transgender, and a female PI, Cooke, with deafness.

G. Project Publications

All publications and presentations of the work funded must be entered in the SCEC Publications database. Log in at *http://www.scec.org/user/login* and select the Publications button to enter the SCEC Publications System. Please either (a) update a publication record you previously submitted or (b) add new publication record(s) as needed. If you have any problems, please email *web@scec.org* for assistance.

II. Technical Report

A. Introduction

Constraining the state of stress along faults prior to previous ground-rupturing earthquakes reveals the conditions that generate these events. Dynamic rupture models show that earthquake behavior varies for different initial stresses (e.g., Douilly et al., 2020; Kame et al., 2003; Lapusta & Liu, 2009). In the absence of data on initial stresses, dynamic models can assume uniform tractions along the faults based on stress levels required to initiate rupture (e.g., Lozos, 2016). However, the tractions along a fault segment on the eve of ground rupturing earthquakes depend on the interseismic stressing rate and time since last event (e.g., Hatch et al., 2020; Smith-Konter & Sandwell, 2009), which may vary spatially along the segment due to the previous rupture history along the faut segment and along nearby segments. Scharer and Yule's (2020) recent compilation of the time and extent of past earthquakes provides estimates of time since last event along nearly all portions of the San Jacinto and southern San Andreas faults over the past 1000 years. This history combined with estimates of interseismic stressing rates and simulations of rupture events enables first order estimates of the fault tractions that accumulate between rupture events. We can provide these estimates using forward models of stress accumulation over the past 1000 years.

While the interseismic stressing rate, time since last event and effects of nearby earthquakes all contribute to the evolution of shear tractions along the San Jacinto (SJf) and San Andreas faults (SAf), the uncertainties of each of these contributors need to be considered. In particular, we run many Monte Carlo realizations that vary event timing, stress drop and inelastic stress relaxation during the interseismic period. With these uncertainties we can bracket probable traction conditions along faults on the eve of past large ruptures. Such estimates will be valuable as initial conditions for dynamic rupture models of these events.

B. Methods

We use 3D Boundary Element Method models to simulate both interseismic stress accumulation and ground rupturing earthquakes within the last 1000 years. The fault geometry of the southern SAf system, based on the SCEC Community Fault Model (Nicholson et al., 2013; Plesch et al., 2007), is represented with triangular elements that can replicate branching and curving fault surfaces. The model includes the San Andreas fault from Parkfield to the Salton Sea, allowing us to simulate 31 events over the past 1000 years. To estimate interseismic loading on the faults, we use an approach that is equivalent to back slip, applying slip rates from a long-term steady state model below a prescribed fault locking depth (e.g., Marshall et al., 2009). For the steady state model, the shear traction-free faults throughout the model slip freely in response to both applied tectonic loading and fault interaction. We prescribe tectonic loading far from the investigated faults at the base of the model to simulate geodetically constrained plate motions, following Herbert & Cooke (2012) and subsequent refinements of Beyer et al. (2018). Additionally, we reduce tectonic loading at the northeast corner of the model to compensate for not including deformation across Walker Lane in the model. Slip rates from the San Gorgonio Pass region of the model match well available geologic rates (e.g., Hatch et al. 2023; Beyer et al. 2018), suggesting the long-term steady state model captures the partitioning of strain along the > 30

active faults in the network. We prescribe tractions from the steady state model below 25 km depth to obtain the interseismic locking depths for each fault element comprising the faults.

To estimate the accumulated tractions prior to ground rupturing earthquakes, we sum the accrued stresses from interseismic loading and the impact of nearby earthquakes. For the interseismic contribution, we multiply the interseismic stressing rate by the time since the fault section last experienced a ground-rupturing earthquake (e.g., Hatch et al., 2020; Smith-Konter & Sandwell, 2009). To simulate the ground rupturing earthquakes on the SJf and SAf, we set up rupture patches for each event based on the compilation of Scharer and Yule (2020).

In this study we investigate the scenario that large ground rupturing earthquakes along the San Andreas and San Jacinto faults relieve a similar stress drop. This may relieve only a portion of the accumulated stress, and can occur if the dynamic strength does not drop to zero during earthquake rupture. Evidence from mapping of strike-slip ruptures suggests that the rupture ends along mature faults have tapering slip (e.g., Barka et al., 2002) that reflects increased resistive stress at the fault ends where friction has not reached fully dynamic sliding values (e.g., Bürgmann et al., 1994; Cooke, 1997). Additionally, slip inversions of ground rupturing earthquakes along mature strike-slip faults show a shallow slip deficit, with slip maxima at ~5 km depth (e.g., Delouis et al., 2002). For our incomplete stress drop models, we use a tapered stress drop distribution that is uniform in the center of the rupture patch and tapers to 0 MPa within 5 km of the surface and 10 km of the lateral rupture tips. We use a ~1 MPa stress drop in the center of the rupture patch based on fit of coseismic simulations to observed displacements for recent rupture events on the SJf and SAf (Anderson-Merritt and Cooke, 2021), which produces an area weighted average stress drop of ~0.75 MPa. We can assess the validity of our assumption that large ground rupturing earthquakes along the San Andreas and San Jacinto faults have consistent stress drop by comparing the slip per event from the simulating events to the slip per event geologic data (Figure 1). The match of slip per event data supports the inference of an overall ~0.75 MPa stress drop for the large ground rupturing earthquakes.
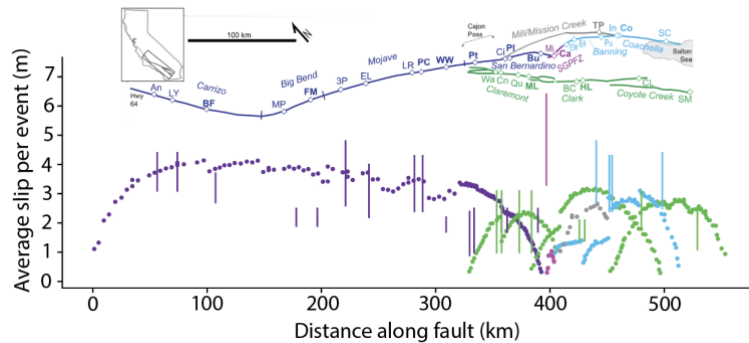

Figure 1: Average slip per event from simulation (dots) and geologic estimates from Scharer and Yule (2021) that were calculated from slip rate and recurrence interval data (vertical lines colored by fault).

While much remains unknown about interseismic stress relaxation off of faults in the crust, abundant evidence of pervasive distributed strain demonstrates that the upper crust relieves stress via processes such as pressure solution creep and microcracking (e.g., Elliott, 1976). We follow the approach of dynamic rupture models (e.g., Duan & Oglesby, 2005) that estimate inelastic interseismic deformation by adjusting the elastically accumulated stresses. We estimate

stress relaxation between earthquakes using a Maxwell solid with effective viscosity, η, that controls the degree of stress relaxation by inelastic processes. Here, we explore the impact of η =10^{19}-10^{21} Pa-sec, which is consistent with estimates of η from long-term geologic observations (Johnson, 2018; Rutter, 1976).

To explore the effect of multiple sources of epistemic uncertainty, we employ a stochastic approach. For each scenario tested, we use 100 Monte Carlo realizations to capture the range of potential stress evolution histories at each of the sites of geologic slip investigations. We use box car uncertainties for the earthquake timing and Gaussian distributions for both stress drop magnitude (mean = ~0.75 MPa, standard deviation = 0.25 MPa) and the exponent of the effective viscosity (mean = 20, standard deviation = 0.5).

C. Results

The accumulated tractions depend on the timing and stress drop of the past events as well as inelastic relaxation of stresses during the interseismic period (Fig. 2). We start the model with zero shear tractions at the time of the last earthquake prior to 1000 CE. If the tractions following the pre-1000 CE earthquake were not zero, the calculated traction values after 1000 CE might be greater (shifted up on Figure 2). For this reason, we do not penalize the prediction of left-lateral tractions within the incomplete stress drop models. Because left-lateral tractions are not expected prior to historical right-lateral ground-rupturing earthquakes, such predictions could provide insight into the absolute tractions on the fault system.

1. Traction evolution

The tractions at sites along the San Andreas and San Jacinto faults increase between events and decrease when a rupture passes through the site. Simulations with η ~10^{21} Pa-s are indistinguishable from the elastic simulations while simulations with η ~10^{19} Pa-s relieve nearly all of the accumulated interseismic stress. Such low viscosity is inconsistent with the record of earthquakes that release seismic energy. While all earthquakes are right-lateral, some portions
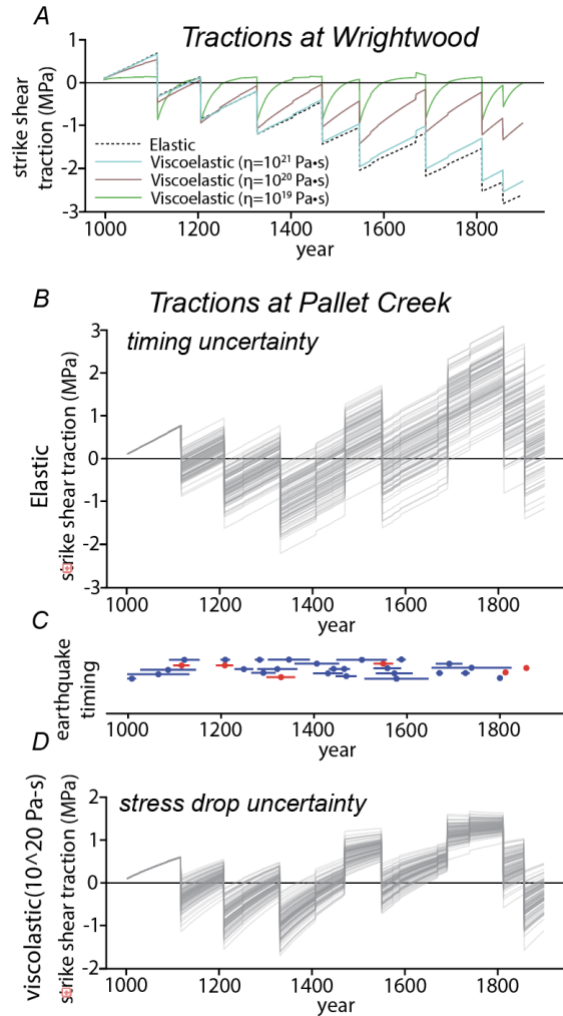

Figure 2: Modeled traction evolution at the Wrightwood (A) and Pallet Creek (B,C & D) sites. A) traction evolution with different crustal viscosity impact stress accumulation in the interseismic period. Monte Carlo simulations with stochastic sampling of (B) earthquake timing in elastic (B) models and (D) stress drop within viscoelastic models. C) shows the earthquake record with red events passing through the site and blue events elsewhere on the fault system.

of the simulations produce left-lateral tractions (negative). Such tractions arise around 1350 at Pallett Creek and for much of the Wrightwood simulation (Figure 2). This suggests that the applied stress drops exceed the accumulated stresses. The stress history of the Wrightwood site is not representative of stress history along the San Andreas and San Jacinto faults sites but raises questions about the stress drops used in the models.

2. Uncertainty of timing, stress drop and viscosity exponent

The uncertainty of earthquake timing produces variability of tractions expressed as the superposition of traction history realizations (Fig. 2 B&D). The timing uncertainty produces uncertainty of tractions ~1 MPa for older events. After recent events with known timing, the traction uncertainty decreases. For events since 1800 the traction uncertainty reflects only the uncertainty in the timing of the pre-1000 CE earthquake. The earthquake timing uncertainties accrue over time resulting in large uncertainty in the accumulated tractions late in the model timeframe. For the Pallett Creek site, present-day strike shear tractions may range from -1 MPa (sinistral) to 1 MPa (dextral). Including interseismic viscoelastic stress relaxation in the assessment of stress drop uncertainty reduces the accumulated tractions and slightly reduces the range of tractions that result from stress drop uncertainty. Consequently, the largest uncertainties in the traction estimates for a given crustal viscosity arise from the values of the coseismic stress drops.

3. Assessment of accumulated stresses on the eve of past earthquakes

We investigate the area-weighted average pre-earthquake tractions on the rupture patch for each simulated earthquake (Figure 3). The elastic model has greater accumulated tractions than the viscoelastic, which rarely exceed ~1 MPa throughout the past 1000 years. The minimum accumulated tractions in the viscoelastic model correlates with rupture length, longer ruptures correlate with greater pre-earthquake tractions. This finding suggests that while large accumulations of shear tractions can produce either short or long ruptures, lesser accumulated traction before the earthquake cannot produce long ruptures.

Many dextral earthquakes occur after the accumulation of sinistral tractions prior to the event. Because we assume complete stress drop on the last event before 1000 CE, all of the accumulated tractions are relative to this event. The non-physical outcome of sinistral tractions before dextral earthquakes
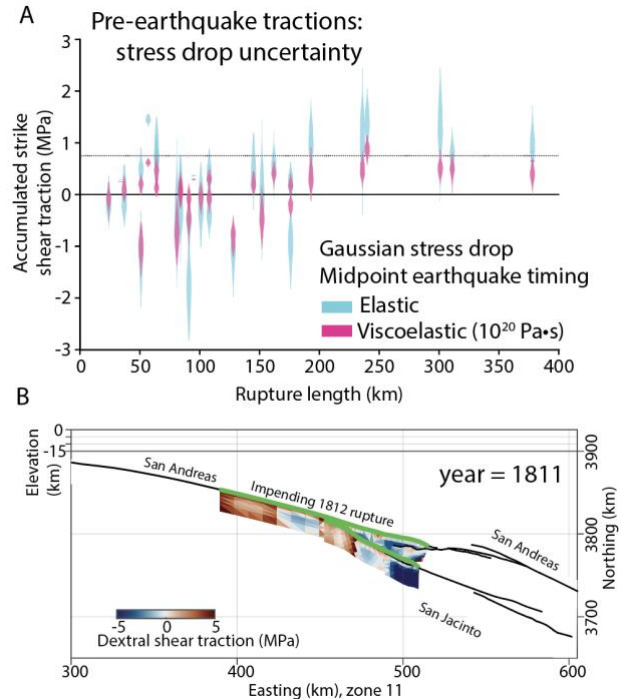

Figure 3: Pre-earthquake tractions from Monte Carlo simulations using elastic and inelastic rheology incomplete stress drop scenarios. Minimum pre-earthquake tractions increase with rupture length.

suggests that the absolute residual shear traction on the faults may be ~1.5 MPa.

D. Conclusions

In this study, we estimate the evolving and pre-earthquake along-strike shear tractions along the San Andreas and San Jacinto faults since ~1000 CE. Models with overall stress drop of ~0.75 MPa produce slip per event that are consistent with geologic data and models with upper crustal viscosity of 10^{20} Pa-sec or greater produce traction histories that are consistent with geologic data We also investigate the impacts of uncertainty in earthquake timing, upper crustal viscosity and stress drop on shear traction estimates. Uncertainties in crustal viscosity have the greater impact on shear tractions followed by stress drop uncertainties. While the earthquake timing uncertainties are large, they do not impact the shear traction estimates as much as other uncertainties. Estimates of the fault shear tractions through time and over several earthquake cycles reveal potential conditions that preceded previous ground-rupturing earthquakes and can provide initial conditions for dynamic rupture models. Our findings show that longer ruptures are associated with greater accumulated shear traction prior to the earthquake.

E. References

Anderson-Merritt, E., & Cooke, M. L. (2021). Estimating tractions along the San Andreas and San Jacinto faults prior to ground-rupturing earthquakes of the last four centuries. In *SCEC Annual Meeting*.

Barka, A., Akyuz, H. S., Altunel, E., Sunal, G., Cakir, Z., Dikbas, A., et al. (2002). The surface rupture and slip distribution of the 17 August 1999 Izmit earthquake (M 7.4), North Anatolian fault. *Bulletin of the Seismological Society of America*, *92*(1), 43–60.

Beyer, J. L., Cooke, M. L., & Marshall, S. T. (2018). Sensitivity of deformation to activity along the Mill Creek and Mission Creek strands of the southern San Andreas fault. *Geosphere*, *14*(6), 2296–2310. https://doi.org/10.1130/GES01666.1

Biasi, G. P., Weldon, R. J., Fumal, T. E., & Seitz, G. G. (2002). Paleoseismic event dating and the conditional probability of large earthquakes on the southern San Andreas fault, California. *Bulletin of the Seismological Society of America*, *92*(7), 2761–2781.

Buga, M. (2012). Paleoseismology of the southern Clark strand of the San Jacinto fault zone, southern California. San Diego, California.

Bürgmann, R., Pollard, D. D., & Martel, S. J. (1994). Slip distributions on faults: effects of stress gradients, inelastic deformation, heterogeneous host-rock stiffness, and fault interaction. *Journal of Structural Geology*, *16*(12), 1675–1690. https://doi.org/10.1016/0191-8141(94)90134-1

Cooke, M. L. (1997). Fracture localization along faults with spatially varying friction. *Journal of Geophysical Research B: Solid Earth*, *102*(B10).

Delouis, B., Giardini, D., Lundgren, P., & Salichon, J. (2002). Joint Inversion of InSAR, GPS, Teleseismic, and Strong-Motion Data for the Spatial and Temporal Distribution of Earthquake Slip: Application to the 1999 İzmit Mainshock. *Bulletin of the Seismological Society of America*, *92*(1), 278–299. https://doi.org/10.1785/0120000806

Douilly, R., Oglesby, D. D., Cooke, M. L., & Hatch, J. L. (2020). Dynamic models of earthquake rupture along branch faults of the eastern San Gorgonio Pass region in California using complex fault structure. *Geosphere*, *16*(2), 474–489.

Duan, B., & Oglesby, D. D. (2005). Multicycle dynamics of nonplanar strike-slip faults. *Journal of Geophysical Research: Solid Earth*, *110*(3), 1–16. https://doi.org/10.1029/2004JB003298

Elliott, D. (1976). The Energy Balance and Deformation Mechanisms of Thrust Sheets Philosophical Transactions of the Royal Society of London . Series A , Mathematical and Physical Sciences , Vol . 283 , No . 1312 , A Discussion on Natural Strain and Geological Structure . (. *Strain*, *283*(1312), 289–312.

Feigl, K. L., Sarti, F., Vadon, H., McClusky, S., Ergintav, S., Durand, P., et al. (2002). Estimating slip distribution for the Izmit mainshock from coseismic GPS, ERS-1, RADARSAT, and SPOT measurements. *Bulletin of the Seismological Society of America*, *92*(1), 138–160.

Fialko, Y. (2004). Probing the mechanical properties of seismically active crust with space geodesy: Study of the coseismic deformation due to the 1992 M_w 7.3 Landers (southern

California) earthquake. *Journal of Geophysical Research*, *109*(B3), B03307. https://doi.org/10.1029/2003JB002756

Fialko, Y., Sandwell, D., Simons, M., & Rosen, P. (2005). Three-dimensional deformation caused by the Bam, Iran, earthquake and the origin of shallow slip deficit. *Nature*, *435*(7040), 295–299. https://doi.org/10.1038/nature03425

Hatch, J. L., Cooke, M. L., Stern, A. R., Douilly, R., & Oglesby, D. D. (2020). Considering fault interaction in estimates of absolute stress along faults in the San Gorgonio Pass region, southern California. *Geosphere*, *16*(3), 751–764. https://doi.org/10.1130/ges02153.1

Herbert, J. W., & Cooke, M. L. (2012). Sensitivity of the Southern San Andreas fault system to tectonic boundary conditions and fault configurations. *Bulletin of the Seismological Society of America*, *102*(5). https://doi.org/10.1785/0120110316

Johnson, K. M. (2018). Growth of Fault-Cored Anticlines by Flexural Slip Folding: Analysis by Boundary Element Modeling. *Journal of Geophysical Research: Solid Earth*, *123*(3), 2426–2447. https://doi.org/10.1002/2017JB014867

Jónsson, S., Zebker, H., Segall, P., & Amelung, F. (2002). Fault slip distribution of the 1999 M w 7.1 Hector Mine, California, earthquake, estimated from satellite radar and GPS measurements. *Bulletin of the Seismological Society of America*, *92*(4), 1377–1389.

Kame, N., Rice, J. R., & Dmowska, R. (2003). Effects of prestress state and rupture velocity on dynamic fault branching. *Journal of Geophysical Research: Solid Earth*, *108*(B5).

Lapusta, N., & Liu, Y. (2009). Three-dimensional boundary integral modeling of spontaneous earthquake sequences and aseismic slip. *Journal of Geophysical Research: Solid Earth*, *114*(B9).

Lozos, J. C. (2016). A case for historic joint rupture of the San Andreas and San Jacinto faults. *Science Advances*, *2*(3), 1–8. https://doi.org/10.1126/sciadv.1500621

Marshall, S. T., Cooke, M. L., & Owen, S. E. (2009). Interseismic deformation associated with three-dimensional faults in the greater Los Angeles region, California. *Journal of Geophysical Research: Solid Earth*, *114*(12). https://doi.org/10.1029/2009JB006439

Nicholson, C., Plesch, A., Sorlien, C., Shaw, J., & Hauksson, E. (2013). Updating the 3D fault set for the Community Fault Model (CFM-v4) and revising its associated fault database. In *Southern California Earthquake Center annual meeting*.

Onderdonk, N. W., McGill, S. F., & Rockwell, T. K. (2015). Short-term variations in slip rate and size of prehistoric earthquakes during the past 2000 years on the northern San Jacinto fault zone, a major plate-boundary structure in southern California. *Lithosphere*, *7*(3), 211–234. https://doi.org/10.1130/L393.1

Pinar, A., Honkura, Y., & Kikuchi, M. (1996). A rupture model for the 1967 Mudurnu Valley, Turkey earthquake and its implication for seismotectonics in the western part of the North Anatolian fault zone. *Geophysical Research Letters*, *23*(1), 29–32.

Plesch, A., Shaw, J. H., Benson, C., Bryant, W. A., Carena, S., Cooke, M., et al. (2007). Community Fault Model (CFM) for southern California. *Bulletin of the Seismological Society of America*, *97*(6). https://doi.org/10.1785/0120050211

Pruitt, A. (2009). *Slip rate on the San Andreas Fault near Littlerock, CA*. Appalachian State University.

Rockwell, T. K., Dawson, T. E., Ben-Horin, J. Y., & Seitz, G. (2015). A 21-event, 4,000-year history of surface ruptures in the Anza seismic gap, San Jacinto Fault, and implications for long-term earthquake production on a major plate boundary fault. *Pure and Applied Geophysics*, *172*(5), 1143–1165.

Rutter, E. H. (1976). A Discussion on natural strain and geological structure - The kinetics of rock deformation by pressure solution. *Philosophical Transactions of the Royal Society of London. Series A, Mathematical and Physical Sciences*, *283*(1312), 203–219. https://doi.org/10.1098/rsta.1976.0079

Salisbury, B. J., Rockwell, T. K., & Buga, M. T. (2017). Paleoseismic Evidence for the 21 April 1918 M w 6.9 Surface Rupture of the Northern Clark Strand of the Central San Jacinto Fault, California. *Bulletin of the Seismological Society of America*, *107*(2), 1027–1032.

Salisbury, J. B., Rockwell, T. K., Middleton, T. J., & Hudnut, K. W. (2012). LiDAR and field observations of slip distribution for the most recent surface ruptures along the central san Jacinto fault. *Bulletin of the Seismological Society of America*, *102*(2), 598–619. https://doi.org/10.1785/0120110068

Scharer, K. M., & Yule, D. (2020). A Maximum Rupture Model for the Southern San Andreas and San Jacinto Faults, California, Derived From Paleoseismic Earthquake Ages: Observations and Limitations. *Geophysical Research Letters*, *47*(15). https://doi.org/10.1029/2020GL088532

Scharer, K. M., Biasi, G. P., & Weldon, R. J. (2011). A reevaluation of the Pallett Creek earthquake chronology based on new AMS radiocarbon dates, San Andreas fault, California. *Journal of Geophysical Research: Solid Earth*, *116*(B12).

Sieh, K. E. (1984). Lateral offsets and revised dates of large prehistoric earthquakes at Pallett Creek, Southern California. *Journal of Geophysical Research*, *89*(B9), 7641–7670. https://doi.org/10.1029/JB089iB09p07641

Smith-Konter, B., & Sandwell, D. (2009). Stress evolution of the San Andreas fault system: Recurrence interval versus locking depth. *Geophysical Research Letters*, *36*(13), 1–5. https://doi.org/10.1029/2009GL037235

Stein, R. S., Dieterich, J. H., & Barka, A. A. (1996). Role of stress triggering in earthquake migration on the North Anatolian Fault. *Physics and Chemistry of the Earth*, *21*(4), 225–230.

Weldon, R., Scharer, K., Fumal, T., & Biasi, G. (2004). Wrightwood and the earthquake cycle: What a long recurrence record tells us about how faults work. *Geological Society of America Today*, *14*(9), 4–10. https://doi.org/10.1130/1052-5173(2004)014<4

Wesson, R. L., & Boyd, O. S. (2007). Stress before and after the 2002 Denali fault earthquake. *Geophysical Research Letters*, *34*(7).